# Robust Transmit Nulling in Wideband Arrays

Peter G. Vouras, *Member, IEEE*, and Trac D. Tran, *Fellow, IEEE*

***Abstract*—The ability to create nulls in the transmit pattern of a phased array antenna has many applications in communication and radar systems, including interference and clutter mitigation. This paper describes the implementation of transmit nulls in wideband arrays through the use of a filter bank inserted behind each array element. The filter bank decimates and partitions the transmit signal into independent subbands and utilizes a tapped delay line (TDL) in each subband to form frequency invariant spatial nulls in the array's transmit pattern. New contributions developed in this paper include an algorithm for determining the TDL coefficients and a novel band partitioning scheme based on principal component filter banks (PCFBs), which is shown to be optimal for minimizing spectral errors if the TDL coefficients are quantized. Numerical techniques are presented for approximating ideal PCFBs using practical paraunitary filter banks (PUFBs) and perfect reconstruction filter banks (PRFBs).**

***Index Terms*—Optimization methods, wideband radar, adaptive arrays, filter bank design.**

## I. Introduction

MODERN adaptive arrays deployed in many radar systems have the ability to place nulls in the receive pattern of the antenna. The nulls attenuate unwanted energy received from external sources such as hostile jammers, unintentional electromagnetic interference, or ambient clutter. These antennas typically transmit with a uniform amplitude weighting across the aperture to maximize main beam gain. However, an increasing body of recent research has developed extensive techniques for creating nulls in the transmit pattern of the antenna as well. The benefit is that the antenna can impose a significant two-way loss on clutter signals. Most transmit nulling algorithms developed to date are for narrowband applications and assume infinite phase and amplitude precision. New contributions described in this paper include a transmit nulling architecture for wideband applications and a band partitioning scheme which allocates more quantization bits to the signal frequency bands with greater energy so as to minimize the random quantization errors which degrade transmit nulling performance.

*Notation:* The following conventions are adopted in terms of notation: Bold-faced characters are used to denote matrices and vectors. $\mathbf{I}$ and $\mathbf{0}$ denote the identity and the null matrices or sub-matrices. $\mathbf{A}^T$, $\mathbf{A}^H$, $\mathrm{tr}[\mathbf{A}]$, $\det[\mathbf{A}]$, $Re[\mathbf{A}]$, and $\|\mathbf{A}\|_2$ denote the transpose, the conjugate transpose, the trace, the determinant, the real part, and the Frobenius norm of $\mathbf{A}$ respectively. Discrete-time scalar or vector sequences and filters are denoted with lower-case letters, for instance $h[n]$ or $\mathbf{x}[n]$, and their z-transform with upper-case letters, such as $H(z)$ or $\mathbf{X}(z)$. When used with matrices of rational functions of the complex variable $z$, $\widetilde{\mathbf{H}}(z)$ will denote the paraconjugate matrix obtained by transposing $\mathbf{H}(z)$, conjugating all the coefficients of the rational functions in $\mathbf{H}(z)$, and replacing $z$ by $z^{-1}$. For a filter $H(z)$, $\widetilde{H}(z)$ denotes the filter whose impulse response is the complex conjugate of the time-reversed impulse response of $H(z)$. The term *Laurent polynomial* describes a finite impulse response (FIR) filter with complex coefficients, such as $H(z) = \sum_{i=n}^{m} h_i z^i$, with possibly both positive and negative powers of $z$. The ring of Laurent polynomials is denoted $C[z, z^{-1}]$ where $C$ is the field of complex numbers. The ring of $N$-dimensional matrices with Laurent polynomial entries is written as $\mathbf{M}(N, C[z, z^{-1}])$. Fields are designated by italicized capital letters as in $F$. A polynomial in the indeterminate $x$ with coefficients in $F$ is denoted $F[x]$. A polynomial in $x$ with coefficients in the ring $C[z, z^{-1}]$ is denoted $C[z, z^{-1}][x]$. The notation $a(x)|b(x)$ signifies that the polynomial $a(x)$ divides $b(x)$.

*1) List of Acronyms:* Acronyms in this paper are provided in the footnote.[1]

### A. Previous Work on Narrowband Transmit Nulling

In most practical radar systems, amplitude and phase control is not available at the array element level. Instead, independent phase commands are applied at each array element to form the desired spatial null. A common algorithm for creating transmit nulls using phase-only weights is described by Day in [1], [2]. Day uses the Moore-Penrose pseudoinverse to compute a minimum norm weight vector with arbitrary amplitude and phase components which satisfy a set of equality constraints on the voltage gain of the adapted array pattern. Next, Day minimizes the sample variance of the computed weight vector to arrive at a phase-only solution. Another popular algorithm for computing array element weights was developed by Dufort in [3]. Dufort postulates interference sources in the desired null directions and computes element weights which maximize the signal-to-interference-plus-noise ratio (SINR) at the output of the array. Steyskal describes a classic algorithm for computing phase-only weights using a perturbation function in [4], [5]. Smith derives a numerical search method for computing phase-only adaptive

Manuscript received November 18, 2013; revised February 27, 2014 and May 20, 2014; accepted May 25, 2014. Date of publication July 01, 2014; date of current version July 15, 2014. The associate editor coordinating the review of this manuscript and approving it for publication was Prof. Xiao-Ping Zhang. This research was conducted under the NRL base program and as part of JHU graduate studies.

P. G. Vouras is with the Naval Research Laboratory, Washington, DC 20375 USA (e-mail: peter.vouras@nrl.navy.mil).

T. D. Tran is with the Electrical and Computer Engineering Department, The Johns Hopkins University, Baltimore, MD 21218-2686 USA (e-mail: trac@jhu.edu).

Digital Object Identifier 10.1109/TSP.2014.2329653

[1]Paraunitary Filter Bank (PUFB, page 1), Perfect Reconstruction Filter Bank (PRFB, page 1), Principal Component Filter Bank (PCFB, page 1), Discrete Fourier Transform Filter Bank (DFTFB, page 5), Signal-to-Interference-plus-Noise-Ratio (SINR, page 1), Tapped Delay Line (TDL, page 1), Mean Square Error (MSE, page 2), Finite Impulse Response (FIR, page 1), Effective Radiated Power (ERP, page 2).

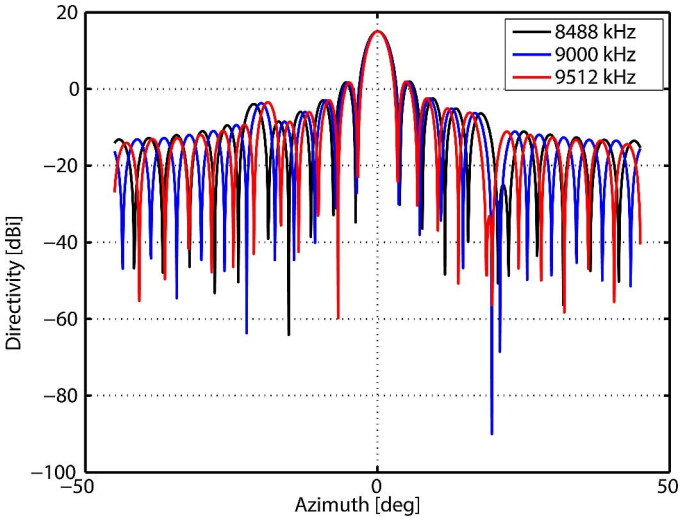


Fig. 1. Frequency cuts of array transmit pattern.

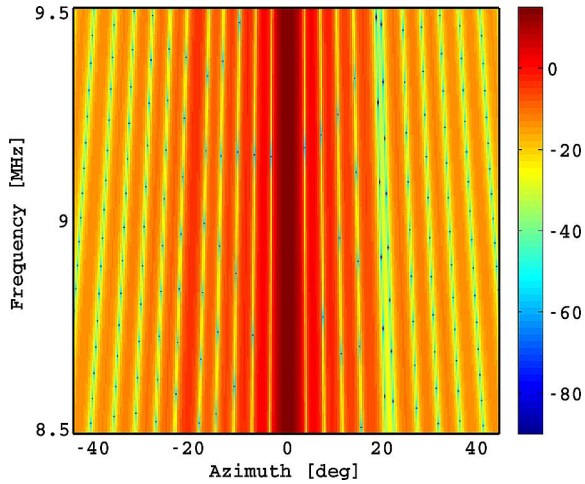


Fig. 2. Array transmit pattern as a function of frequency.

weights based on conjugate gradient optimization and Newton's method in [6].

### B. Wideband Problem Description

Typically, the phase weights applied at each array element are only computed for the center frequency of the array, which corresponds to half-wavelength spacing between the elements. Furthermore, the phase shifter behind each element is only calibrated for the array center frequency. Therefore, the actual phase shift at each array element deviates from the desired value for frequencies other than the array center frequency. As a result, the transmit null changes pointing direction over the entire signal bandwidth.

To illustrate the impact of signal bandwidth on transmit nulls, consider Fig. 1 which shows a phase-only null computed using Smith's algorithm for a uniform linear array with 32 elements [6]. The plot shows a deep null in the desired direction of 19.57° azimuth at the array center frequency of 9 MHz. For this example an ideal array is assumed with no random noise or errors present so the null depth is essentially infinite. The pointing direction of the null clearly changes with frequency, as is also seen in the frequency dependent array pattern of Fig. 2 where the color bar corresponds to directivity in dBi. The yellow line at 19.57° corresponds to the transmit null and the frequency dependent slope of the line indicates that the direction of the null is a function of frequency.

### C. Previous Filter Bank Applications to Wideband Arrays

Filterbank designs have been used extensively in wideband adaptive arrays for frequency invariant beamforming and in sidelobe cancellers to mitigate wideband interference. Zhao in [7] creates frequency invariant beam patterns by partitioning the signal at each array element into subbands and implementing independent beamformers in each subband. Subband adaptive processing using filter banks is also employed in [8] by Zhang to mitigate intersymbol and cochannel interference in digital communications. Compton describes nulling performance on receive for a band partitioned adaptive array in [9]. Lin presents measured data from an experimental wideband canceller testbed with band partitioning in [10]. Weiss explores the use of oversampled filter banks for broadband adaptive beamforming in [11]. The use of linear phase paraunitary filterbanks in wideband adaptive arrays is described in [12].

### D. Overall Technical Approach and Performance Metrics

This paper presents two new algorithms for computing complex element weights that form frequency invariant nulls in an array's transmit pattern. Both algorithms are suitable for wideband arrays but one algorithm employs band partitioning to reduce the sampling rate required in practical implementations. For narrowband arrays, the figure of merit used for transmit nulling performance is null depth. Null depth is defined as the magnitude squared of the array voltage pattern in the direction of the null at the center frequency of the array. For the wideband case with signal energy uniformly distributed over the instantaneous transmit bandwidth the performance metric is null depth averaged over the signal bandwidth. For the most general case with signal energy not uniformly distributed over the entire instantaneous bandwidth, the chosen figure of merit is the Effective Radiated Power (ERP) of the array in the null direction averaged over the signal bandwidth. ERP is also used to compare transmit nulling performance in the presence of quantization errors. Section V shows that a band partitioning scheme adapted to the spectrum of the transmit signal is optimal for minimizing the effect of quantization errors. Two algorithms are presented for designing FIR filter banks that approximate the transfer function of the desired ideal filter bank. Both algorithms minimize the mean square error (MSE) between the ideal filter bank and the approximation. An alternative approach to designing an array band partitioning scheme is to directly optimize the filter bank coefficients so as to yield the lowest possible ERP in the desired null direction. This approach is not considered here due to the much greater complexity of the objective function.

## II. Wideband Array Architecture

A tapped delay line (TDL) is equivalent to a discrete-time FIR filter with unity sample delay between the filter coefficients.

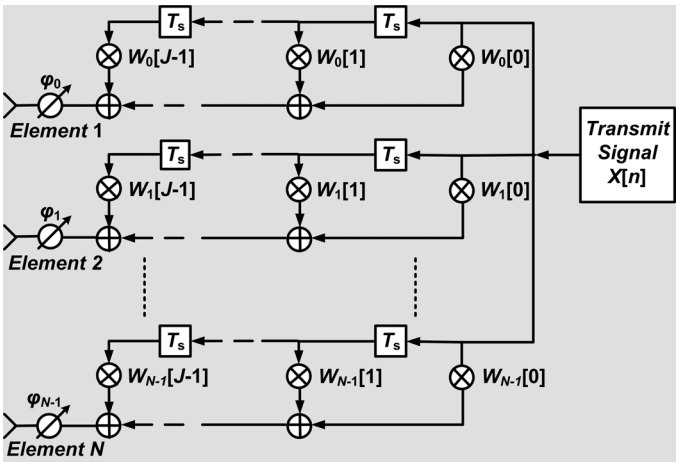


Fig. 3. Wideband array architecture.

Fig. 3 illustrates the proposed TDL architecture for forming frequency invariant transmit nulls in wideband arrays. This architecture does not implement any band partitioning.

Behind each of the $N$ array elements is a TDL with $J$ real taps spaced $T_s$ seconds apart. The response of a TDL array can be written as [13]

$$H(\omega,\theta)=\sum_{m=0}^{J-1}e^{-jm\omega T_s}\sum_{n=0}^{N-1}w_n[m]e^{-jn\phi} \tag{1}$$

where $w_n[m]$ is the $m$th tap coefficient of the $n$th array element, and $\phi$ is the phase difference between adjacent array elements given by

$$\phi=\frac{2\pi D\sin\theta}{\lambda}. \tag{2}$$

The parameter $D$ is the distance between array elements, $\lambda$ is the wavelength of the transmitted signal, and $\theta$ is the main beam steering direction with respect to array normal. If the highest transmit frequency of interest is $f_1$, then $D$ is chosen to be $\lambda_1/2$ to avoid spatial aliasing and $T_s$ is chosen to be $1/(2f_1)$ to avoid temporal aliasing.

### A. Objective Function

To compute the TDL coefficients for a wideband null, the SINR integrated over the signal bandwidth of interest for a hypothetical interference source in the direction of the desired null is maximized. This objective function is derived as follows.

Define a frequency dependent steering vector in the direction $\theta$ for a linear array with $N$ isotropic elements as

$$\mathbf{v}(\theta,f)=\left[v_0(\theta,f),v_1(\theta,f),\ldots,v_{N-1}(\theta,f)\right]^{\mathbf{T}}, \tag{3}$$

where each component in (3) is given by

$$v_n(\theta,f)=\exp\left(j2\pi D(f/c)n\sin\theta\right),\ n=0,\ldots,N-1 \tag{4}$$

with $D$ equal to the inter-element spacing, $f$ the transmit signal frequency, $\theta$ the steering angle of the signal with respect to array normal, and $c$ the speed of light in free space. A vector $\mathbf{w}$ of frequency dependent weights to be applied to each array element is defined as

$$\mathbf{w}(f)=\left[w_0(f),w_1(f),\ldots,w_{N-1}(f)\right]^{\mathbf{T}} \tag{5}$$

where $w_j(f)$ is the frequency response of the $j$th TDL $h_j[k]$ and

$$w_j(f)=\sum_{k=0}^{J-1}h_j[k]e^{-j\omega T_s k}. \tag{6}$$

The frequency dependent signal $\mathbf{R}_{vv}$ and noise $\mathbf{N}_{vv}$ covariance matrices can be written for the main beam steering direction $\theta$ and the direction $\theta_1$ of the desired null as

$$\mathbf{R}_{vv}(f)=\mathbf{v}(\theta,f)\mathbf{v}(\theta,f)^{\mathbf{H}}, \tag{7}$$

$$\mathbf{N}_{vv}(f)=\beta\mathbf{v}(\theta_1,f)\mathbf{v}(\theta_1,f)^{\mathbf{H}}+\sigma^2\mathbf{I}, \tag{8}$$

where $\sigma^2$ is the power of a zero mean additive white noise Gaussian process, and $\beta$ is a real positive scalar. The cost function to be maximized over the signal bandwidth of interest is the integrated SINR

$$\boldsymbol{\xi}=\int_{f_0}^{f_1}\frac{\mathbf{w}^{\mathbf{H}}(f)\mathbf{R}_{vv}(f)\mathbf{w}(f)}{\mathbf{w}^{\mathbf{H}}(f)\mathbf{N}_{vv}(f)\mathbf{w}(f)}W(f)df, \tag{9}$$

where $f_0$ and $f_1$ are the frequency endpoints of the signal bandwidth and $W(f)$ is a nonnegative real scalar weighting function. The metric used to gauge nulling performance is the average null depth $d$ over the bandwidth of interest, defined as

$$d=\frac{1}{P}\sum_{k=0}^{P-1}\left|V(f_k,\theta_1)\right|^2, \tag{10}$$

where $P$ is the number of frequency samples within the signal bandwidth, $\theta_1$ is the desired null location, and $V(f,\theta_1)$ is the frequency dependent array voltage pattern; $V(f,\theta_1)=\sum_{n=0}^{N-1}v_n(\theta_1,f)$. For the case where $Q$ nulls in the array pattern are desired, the noise covariance matrix is written as

$$\mathbf{N}_{vv}(f)=\beta\sum_{j=1}^{Q}\mathbf{v}(\theta_j,f)\mathbf{v}(\theta_j,f)^{\mathbf{H}}+\sigma^2\mathbf{I}. \tag{11}$$

### B. Gradient Computation

To maximize the integrated SINR $\xi$, the conjugate gradient algorithm may be used. This algorithm requires computing the gradient of $\xi$ with respect to the TDL coefficients. Define the matrix $\mathbf{W}$ of TDL coefficients for $N$ array elements with $J$ taps each and the delay chain vector $\mathbf{e}(f)$ by

$$\mathbf{W}=\begin{bmatrix}h_0[0] & h_0[1] & \cdots & h_0[J-1]\\ h_1[0] & h_1[1] & \cdots & h_1[J-1]\\ \vdots & \vdots & \ddots & \vdots\\ h_{N-1}[0] & h_{N-1}[1] & \cdots & h_{N-1}[J-1]\end{bmatrix}, \tag{12}$$

and

$$\mathbf{e}(f)=\left[1,e^{-j2\pi fT_s},\ldots,e^{-j2\pi fT_s(J-1)}\right]^{\mathbf{T}}. \tag{13}$$

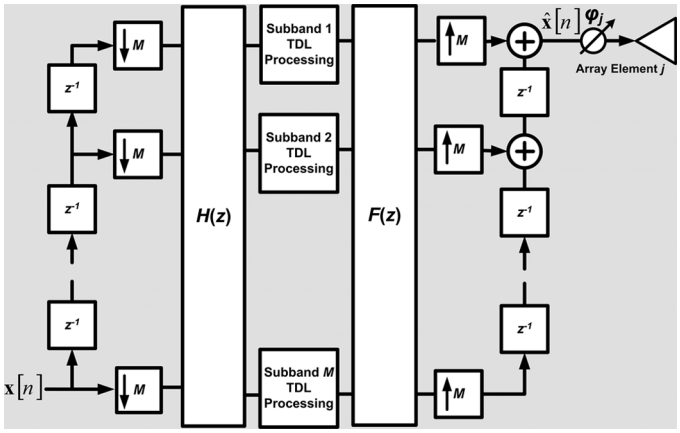


Fig. 4. Array element with band partitioning.

Then

$$\mathbf{w}(f) = \mathbf{W}\mathbf{e}(f). \tag{14}$$

The gradient of $\xi$ with respect to $\mathbf{W}$ can be computed by taking the partial derivatives of $\xi$ with respect to $h_k[j]$ (denoted $h_{kj}$) as

$$\nabla\xi_{kj} = \frac{\partial}{\partial h_{kj}} \int_{f_0}^{f_1} \frac{\mathbf{w}^{\mathbf{H}}(f)\mathbf{R}_{vv}(f)\mathbf{w}(f)}{\mathbf{w}^{\mathbf{H}}(f)\mathbf{N}_{vv}(f)\mathbf{w}(f)} W(f)df, \tag{15}$$

with $0 \leq j \leq J-1$ and $0 \leq k \leq N-1$. For simplicity, assume $W(f) = 1$. By the Dominated Convergence Theorem [14], the partial derivative may be brought inside the integral to yield

$$\nabla\xi_{kj} = \int_{f_0}^{f_1} \frac{\partial}{\partial h_{kj}} \frac{\mathbf{e}^{\mathbf{H}}\mathbf{W}^{\mathbf{H}}\mathbf{R}_{vv}\mathbf{W}\mathbf{e}}{\mathbf{e}^{\mathbf{H}}\mathbf{W}^{\mathbf{H}}\mathbf{N}_{vv}\mathbf{W}\mathbf{e}} df, \tag{16}$$

where the frequency argument $f$ is suppressed.

Useful relations for a matrix $\mathbf{X}$ and vectors $\mathbf{a}$ and $\mathbf{b}$ are

$$\frac{\partial}{\partial \mathbf{X}}\mathbf{a}^{\mathbf{H}}\mathbf{X}\mathbf{b} = \bar{\mathbf{a}}\mathbf{b}^{\mathbf{T}}, \quad \frac{\partial}{\partial \mathbf{X}}\mathbf{a}^{\mathbf{H}}\mathbf{X}^{\mathbf{H}}\mathbf{b} = \mathbf{b}\mathbf{a}^{\mathbf{H}}, \tag{17}$$

where the overbar denotes complex conjugation. These relations and the fact that the matrices $\mathbf{R}_{vv}$ and $\mathbf{N}_{vv}$ are Hermitian yield the derivatives

$$\frac{\partial}{\partial \mathbf{W}}\mathbf{e}^{\mathbf{H}}\mathbf{W}^{\mathbf{H}}\mathbf{R}_{vv}\mathbf{W}\mathbf{e} = 2Re\left\{\mathbf{R}_{vv}\mathbf{W}\mathbf{e}\mathbf{e}^{\mathbf{H}}\right\}, \tag{18}$$

$$\frac{\partial}{\partial \mathbf{W}}\mathbf{e}^{\mathbf{H}}\mathbf{W}^{\mathbf{H}}\mathbf{N}_{vv}\mathbf{W}\mathbf{e} = 2Re\left\{\mathbf{N}_{vv}\mathbf{W}\mathbf{e}\mathbf{e}^{\mathbf{H}}\right\}. \tag{19}$$

Next using the quotient rule yields

$$\nabla\xi_{\mathbf{W}} = \int_{f_0}^{f_1} \frac{\mathbf{\Gamma}(f)}{\delta(f)} df, \tag{20}$$

where

$$\mathbf{\Gamma}(f) = \left(\mathbf{e}^{\mathbf{H}}\mathbf{W}^{\mathbf{H}}\mathbf{N}_{vv}\mathbf{W}\mathbf{e}\right)\left(2Re\left\{\mathbf{R}_{vv}\mathbf{W}\mathbf{e}\mathbf{e}^{\mathbf{H}}\right\}\right) - \left(\mathbf{e}^{\mathbf{H}}\mathbf{W}^{\mathbf{H}}\mathbf{R}_{vv}\mathbf{W}\mathbf{e}\right)\left(2Re\left\{\mathbf{N}_{vv}\mathbf{W}\mathbf{e}\mathbf{e}^{\mathbf{H}}\right\}\right) \tag{21}$$

and

$$\delta(f) = \left(\mathbf{e}^{\mathbf{H}}\mathbf{W}^{\mathbf{H}}\mathbf{N}_{vv}\mathbf{W}\mathbf{e}\right)^2. \tag{22}$$

### C. Conjugate Gradient Algorithm

The stated optimization objective is to maximize $\xi$ over all $\mathbf{W}$. Equivalently, the reciprocal $1/\xi$ may be minimized. The pseudocode for implementing the unconstrained minimization program using a conjugate gradient algorithm is presented in Algorithm 1. The objective function $\xi$, or $1/\xi$, will in general have many local maxima or minima and the final solution will depend to some degree on the initial condition chosen for the algorithm. A suitable initial condition for $\mathbf{W}$ which yields reasonable results is to set the TDL for each array element equal to an arbitrary Type-1 FIR filter.

**Algorithm 1:** Algorithm to Compute TDL Coefficients

**Require:** Initial TDL coefficients $\mathbf{W}_0$. Possible initial condition for each TDL is an arbitrary Type-1 FIR filter with linear phase.

1: $\mathbf{h}_0 = -\nabla\xi_{\mathbf{W}}(\mathbf{W}_0)$
2: $\mathbf{g}_0 = \mathbf{h}_0$
3: For each iteration $j = 0, 1, \ldots$ compute a step size $\lambda_j$ using any line optimization routine. Alternatively, set $\lambda_j$ to a small value that ensures convergence.
4: $\mathbf{W}_{j+1} = \mathbf{W}_j + \lambda_j \mathbf{h}_j$
5: $\mathbf{g}_{j+1} = -\nabla\xi_{\mathbf{W}}(\mathbf{W}_{j+1})$
6: $\mu_j = \frac{(\mathbf{g}_{j+1} - \mathbf{g}_j)^{\mathbf{T}}\mathbf{g}_{j+1}}{\|\mathbf{g}_j\|^2}$
7: $\mathbf{h}_{j+1} = \mathbf{g}_{j+1} + \mu_j \mathbf{h}_j$
8: $j = j + 1$
9: **Go to** 3

## III. Band Partitioning

A drawback to the TDL array architecture shown in Fig. 3 is the high sampling frequency $f_s$ associated with the inter-tap delays. Recall $f_s$ was chosen in (1) to prevent aliasing. The TDL filtering can be performed at a lower sampling rate by partitioning the transmit signal into independent subbands using a filter bank behind each array element. A maximally decimated filter bank with $M$ channels will decimate the input sampling frequency by a factor of $M$, which yields the lowest possible sampling frequency in each channel. Fig. 4 illustrates the polyphase structure of a maximally decimated filter bank behind one array element. Desirable filter banks for a wideband array are paraunitary filter banks (PUFBs) or more general perfect reconstruction filter banks (PRFBs) since they preserve the input signal in the absence of any subband processing. Oversampled filter banks have also received some attention in wideband beamforming [11]. However, with oversampled filter banks the decimation factor is less than the number of frequency channels so these filter banks will not be considered here.

### A. Paraunitary Filter Banks

Consider a maximally decimated filter bank with $M$ channels and a subband decimation factor equal to $M$. Each analysis filter $H_k(z)$ with impulse response $h_k(n)$ can be expressed in terms of its polyphase components as

$$H_k(z) = \sum_{l=0}^{M-1} z^{-l} E_{kl}\left(z^M\right), \quad k = 0, 1, \ldots, M-1 \tag{23}$$

where $e_{kl}[n] = h_k[l + Mn]$ for $0 \le l \le M-1$ and

$$E_{kl}(z) = \sum_{n=-\infty}^{\infty} e_{kl}[n] z^{-n}. \tag{24}$$

The entire bank of analysis filters can be written as

$$\mathbf{h}(z) = \mathbf{H}(z^M)\mathbf{e}(z), \tag{25}$$

where the transfer function vector $\mathbf{h}(z)$ and the delay chain vector $\mathbf{e}(z)$ are defined to be

$$\mathbf{h}(z) = \begin{bmatrix} H_0(z) \\ H_1(z) \\ \vdots \\ H_{M-1}(z) \end{bmatrix}, \quad \mathbf{e}(z) = \begin{bmatrix} 1 \\ z^{-1} \\ \vdots \\ z^{-(M-1)} \end{bmatrix}. \tag{26}$$

The $M$-by-$M$ polyphase component matrix is $\mathbf{H}(z) = [E_{kl}(z)]$. Based on the polyphase representations of analysis and synthesis filters, a filter bank may be efficiently implemented as shown in Fig. 4.

Paraunitary (orthonormal) polyphase matrices satisfy the conditions,

$$\widetilde{\mathbf{H}}(z)\mathbf{H}(z) = \mathbf{H}(z)\widetilde{\mathbf{H}}(z) = c^2\mathbf{I}, \quad \widetilde{\mathbf{H}}(z) = \mathbf{H}^{\mathbf{H}}(1/\overline{z}), \tag{27}$$

where the overbar denotes conjugation and the complex variable $z = re^{j\omega}$. Causal and stable paraunitary polyphase matrices are unitary on the unit circle, meaning $\mathbf{H}^{-1}(e^{j\omega}) = \mathbf{H}^{\mathbf{H}}(e^{j\omega})$. The analysis filters $h_k[n]$ and the synthesis filters $f_k[n]$ of length $L$ in a paraunitary filter bank are related as

$$f_k[n] = c\overline{h}_k[L-n], \qquad F_k(z) = cz^{-L}\widetilde{H_k}(z). \tag{28}$$

In other words, the impulse response of the synthesis filters of a PUFB can be obtained by conjugating and time-reversing the coefficients of the analysis filters. The analysis and synthesis filters of a PUFB will have the same magnitude response up to a scaling factor [15].

### B. Discrete Fourier Transform Filter Bank

Two similar filter banks used extensively in signal processing applications are the Discrete Fourier Transform Filter Bank (DFTFB) and the Discrete Cosine Transform Filter Bank [16]. Neither filter bank allows for any optimized filter design and both filter banks uniformly partition the signal spectrum. Therefore, only the DFTFB will be considered here.

The DFTFB is a maximally decimated FIR paraunitary system with a bank of $M$ analysis filters that are uniformly shifted versions of a lowpass prototype filter $H_0(z)$. In other words,

$$H_k(z) = H_0(zW^k), \tag{29}$$

where $W = e^{-j2\pi/M}$ and

$$H_0(z) = 1 + z^{-1} + \cdots + z^{-(M-1)}. \tag{30}$$

Notice that the filters have length $M$, which is equal to the number of channels. The analysis polyphase matrix $\mathbf{H}(z) = \overline{\mathbf{W}}$, where $\mathbf{W}$ is the $M$-by-$M$ DFT matrix with elements $[\mathbf{W}]_{km} = W^{km}$. The synthesis polyphase matrix $\mathbf{F}(z)$ is given by $\mathbf{F}(z) = \mathbf{W}$ and the reconstructed signal at the output of the filter bank is

$$\widehat{x}[n] = Mx[n - M + 1], \tag{31}$$

which is simply a delayed version of the input. The synthesis filters are related by

$$F_k(z) = W^{-k}F_0(zW^k), \tag{32}$$

where $F_0(z) = H_0(z)$. Thus each synthesis filter has the same magnitude response as the corresponding analysis filter (see [15, p. 241], [16, p. 300]).

### C. Band Partitioned Transmit Nulling Algorithm

The proposed nulling algorithm for a band-partitioned array architecture is similar to the algorithm previously described in Section II. The only differences are that the optimization objective must be maximized independently for each subband and the scalar weighting function $W(f)$ in (9) is set equal to the composite magnitude response of the analysis and synthesis filters in each channel, i.e., $W(f) = |H_j(f)F_j(f)|$. Thus, the objective function to be maximized in the $j$th subband becomes

$$\boldsymbol{\xi}_j = \int_{f_0}^{f_1} \frac{\mathbf{w}_j^{\mathbf{H}}(f)\mathbf{R}_{vv}(f)\mathbf{w}_j(f)}{\mathbf{w}_j^{\mathbf{H}}(f)\mathbf{N}_{vv}(f)\mathbf{w}_j(f)} \left|H_j(f)F_j(f)\right| df. \tag{33}$$

This objective may also be maximized using the conjugate gradient algorithm previously described, after the gradient vector in (20) has been modified to include the new weighting function via

$$\nabla\xi_{\mathbf{W}} = \int_{f_0}^{f_1} \frac{\boldsymbol{\Gamma}(f)\left|H_j(f)F_j(f)\right|}{\delta(f)} df. \tag{34}$$

## IV. TDL Coefficient Quantization

For transmit nulling operation in any practical radar system with hundreds or perhaps thousands of elements, it is not feasible to compute the TDL coefficients in real-time. Instead, the TDL coefficients must be pre-computed and retrieved from a look-up table. The resulting number of data points in the table could be substantial if it accounts for every possible combination of main beam and null pointing directions. To reduce the memory footprint of such a scheme, the TDL coefficients must be quantized and stored in fixed precision using as few bits as possible. The effect of such an implementation on nulling performance is to introduce errors in the frequency response of each TDL. These errors in turn will degrade the depth of the transmit null. Quantizing the TDL coefficients to a range of discrete values can be modeled by adding random quantization noise to each infinite precision coefficient. The quantization noise is assumed to be independent between bins of the quantizer.

Assume a $B$-bit quantizer is used to represent the computed TDL coefficients in finite precision. The output of the quantizer can be modeled by adding random errors $e[n]$ to the real TDL coefficients $h[n]$. If $-1 \le h[n] \le 1$, then the smallest quanta at the output of the quantizer is $1/2^B$, and the quantization errors

will be uniformly distributed in the interval $[-1/2^{B+1}, 1/2^{B+1}]$ with a variance of $2^{-2B}/12$ [17].

### A. Quantization Effects on TDL Frequency Response

If the TDL coefficients in each subband are stored in fixed precision, the TDL frequency response will differ from ideal. It is possible to derive an upper bound for the error in the magnitude squared response of a TDL due to coefficient quantization. Let $D(\theta)$ denote a desired TDL frequency response, where $0 \leq \theta \leq 2\pi$ is normalized frequency (i.e., the sampling frequency corresponds to $2\pi$). Assume a direct realization of the TDL using coefficients $\mathbf{b} = [b[0], b[1], \ldots, b[J-1]]^{\mathbf{T}}$. The quantized parameters $\mathbf{p} = [p[0], p[1], \ldots, p[J-1]]^{\mathbf{T}}$ are obtained by adding quantization errors $e[k]$ to the ideal coefficients $b[k]$ as in

$$p[k] = b[k] + e[k], \quad k = 0, 1, \ldots, J-1. \tag{35}$$

Let $T(\theta)$ represent the frequency response of the quantized TDL. Then using a Taylor Series Expansion yields

$$|T(\theta)|^2 \approx |D(\theta)|^2 + \nabla_{\mathbf{b}} \left(|D(\theta)|^2\right)^{\mathbf{T}} (\mathbf{p} - \mathbf{b}), \tag{36}$$

where

$$D(\theta) = \sum_{k=0}^{J-1} b[k] e^{-j\theta k}, \quad T(\theta) = \sum_{k=0}^{J-1} p[k] e^{-j\theta k}. \tag{37}$$

Thus,

$$|T(\theta)|^2 - |D(\theta)|^2 \approx \sum_{k=0}^{J-1} \frac{\partial |D(\theta)|^2}{\partial b[k]} (p[k] - b[k]). \tag{38}$$

Using the derivative formulas

$$\frac{\partial D(\theta)}{\partial b[k]} = \frac{\partial T(\theta)}{\partial p[k]} = e^{-j\theta k} \tag{39}$$

and the product rule for differentiation yields

$$\frac{\partial |D(\theta)|^2}{\partial b[k]} = 2Re\left\{e^{j\theta k} D(\theta)\right\}. \tag{40}$$

Let $L$ denote the full scale value used for the coefficient $b[k]$. One way of choosing the full scale value is to find the coefficient having the largest magnitude from all the TDLs and use it as the full scale value for all the coefficients [18]. In other words,

$$L = \max_{k,j,l} |b_{lj}[k]| \tag{41}$$

for $0 \leq k \leq J-1, 0 \leq j \leq M-1, 0 \leq l \leq N-1$ where the index $k$ varies across all taps, $j$ varies across all subbands, and $l$ varies across all array elements. Then

$$|p[k] - b[k]| \leq Lq \tag{42}$$

where $q = 2^{-B}$ and $B$ is the number of quantizer bits. Thus,

$$\begin{aligned} \left||T(\theta)|^2 - |D(\theta)|^2\right| &\leq q \sum_{k=0}^{J-1} \left| \frac{\partial |D(\theta)|^2}{\partial b[k]} \right| L \\ &\leq 2^{-B+1} \sum_{k=0}^{J-1} |D(\theta)| L. \end{aligned} \tag{43}$$

Since any TDL is stable and has finite coefficients, there exists a finite constant $D_{MAX}$ such that

$$|D(\theta)| \leq \sum_{k=0}^{J-1} |b[k]| \leq D_{MAX} \tag{44}$$

for any TDL in any subband of any array element. Thus,

$$\left||T(\theta)|^2 - |D(\theta)|^2\right| \leq 2^{-B+1} \sum_{k=0}^{J-1} D_{MAX} L \leq 2^{-B+1} \Phi, \tag{45}$$

where $\Phi = LJD_{MAX}$.

Let the input $v_j$ to the TDL $\mathbf{p}_j$ in the $j$th subband be a zero-mean wide-sense–stationary (WSS) process with power spectral density (psd) $S_{v_j v_j}(\theta)$. The absolute difference between the output of an ideal TDL with coefficients of infinite precision and the output of a quantized TDL is the spectral error $\epsilon_j(\theta)$,

$$\epsilon_j(\theta) = S_{v_j v_j}(\theta) \left||T(\theta)|^2 - |D(\theta)|^2\right|. \tag{46}$$

An upper bound for $\epsilon_j(\theta)$ is

$$\epsilon_j(\theta) \leq S_{v_j v_j}(\theta) 2^{-B+1} \Phi. \tag{47}$$

Note that this upper bound holds for all the TDLs in the array and that the constant $\Phi$ can be taken to be independent of the band-partitioning scheme in any filter bank. Integrating $\epsilon_j(\theta)$ over all frequencies yields

$$\frac{1}{2\pi} \int_0^{2\pi} \epsilon_j(\theta) d\theta \leq \Phi 2^{-B+1} {\sigma_j}^2 \equiv \Psi_j, \tag{48}$$

where the variance ${\sigma_j}^2$ of $v_j$ is

$${\sigma_j}^2 = \frac{1}{2\pi} \int_0^{2\pi} S_{v_j v_j}(\theta) d\theta. \tag{49}$$

The quantity $\Psi_j$ represents an upper bound on the average power of the spectral error in the $j$th subband. Thus, the impact of TDL quantization on null depth can be mitigated by minimizing the sum of $\Psi_j$ over all $M$ subbands. Since the factor $2\Phi$ does not affect the minimization, it may be dropped. Consequently, the criterion for minimizing TDL quantization effects reduces to finding a filter bank from the class of paraunitary filter banks that minimizes the objective function

$$\eta = \sum_{j=0}^{M-1} 2^{-B_j} {\sigma_j}^2, \tag{50}$$

where $B_j$ is the number of quantization bits allocated to the $j$th subband. Notice the minimization objective is purely a function of the subband variances. The optimal filter bank for this problem is described in the next section.

## V. Principal Component Filter Banks

*Definition*

Principal Component Filter Banks (PCFBs) have been studied extensively in the literature and discovered to be optimal for a variety of applications, including maximizing the coding gain in data compression applications [19]–[21]. In this section, PCFBs are also shown to be optimal for minimizing the signal errors at the output of a paraunitary filter bank due to subband processing with quantized TDLs. PCFBs have the property that most of the signal energy is packed into the first subband, the second most energy into the second subband, and so on. Consequently, by assigning a greater number of quantization bits to the subbands with greater signal energy, the overall impact of quantization errors can be reduced at the output of the filter bank.

Let ${\sigma_j}^2$ denote the variance of the $j$th subband signal produced by feeding the scalar signal $x[n]$ to the input of the filter bank. To every possible filter bank within the class of paraunitary filter banks, there corresponds a subband variance vector $\boldsymbol{\sigma}^2$. Let $\mathbf{x}[n]$ denote the $M$-fold blocked version of $x[n]$ given by $\mathbf{x}[n] = [x[n], x[n-1], \ldots, x[n-M+1]]^{\mathbf{T}}$. The vector $\mathbf{x}[n]$ is a WSS process with psd matrix $\mathbf{S}_{xx}(e^{j\omega})$. The subband variance vector associated with $x[n]$ is defined as the vector $\boldsymbol{\sigma}^2 = \left[{\sigma_0}^2, {\sigma_1}^2, \ldots, {\sigma_{M-1}}^2\right]^{\mathbf{T}}$. Given the analysis polyphase matrix $\mathbf{H}(e^{j\omega})$ of a PUFB and $\mathbf{S}_{xx}(e^{j\omega})$, the subband variance vector can be computed as [21]

$$\boldsymbol{\sigma}^2 = \frac{1}{2\pi}\int_0^{2\pi} \operatorname{diag}\left(\mathbf{H}(e^{j\omega})\mathbf{S}_{xx}(e^{j\omega})\mathbf{H}^{\mathbf{H}}(e^{j\omega})\right) d\omega. \quad (51)$$

The optimization search space corresponding to the objective function in (50) is defined to be the set of all subband variance vectors corresponding to all filter banks in the class $\mathcal{C}$ of PUFBs. A filter bank in $\mathcal{C}$ is said to be a PCFB for $\mathcal{C}$ and $\mathbf{S}_{xx}(e^{j\omega})$ if its subband variance vector majorizes the subband variance vector of every other filter bank in $\mathcal{C}$ [21].

### A. Optimality

The optimality of PCFBs for a variety of band-partitioning applications is derived from an important property referred to as majorization. Consider two sets $A$ and $B$, each with $M$ real numbers: $A = \{a_0, a_1, \ldots, a_{M-1}\}$ and $B = \{b_0, b_1, \ldots, b_{M-1}\}$. The set $A$ is said to majorize the set $B$ if the elements of these sets, when ordered such that $a_0 \geq a_1 \geq \cdots \geq a_{M-1}$ and $b_0 \geq b_1 \geq \cdots \geq b_{M-1}$, obey the property

$$\sum_{j=0}^{P} a_j \geq \sum_{j=0}^{P} b_j \quad (52)$$

for all $P = 0, 1, \ldots, M-1$, with equality holding when $P = M-1$. Given two real-valued vectors $\mathbf{a}$ and $\mathbf{b}$, $\mathbf{a}$ is said to majorize $\mathbf{b}$ when the set of components of $\mathbf{a}$ majorizes that of $\mathbf{b}$. Any permutation of $\mathbf{a}$ will also majorize any permutation of $\mathbf{b}$. The majorization property of PCFBs can be used to prove the following claim, which is a central contribution of this paper.

*1) Claim 1:* Among all paraunitary filter banks, the filter bank which minimizes the objective function $\eta$ given in (50) is a PCFB.

*Proof:* Label the filter bank channels such that ${\sigma_0}^2 \geq {\sigma_1}^2 \geq \cdots \geq {\sigma_{M-1}}^2$. Next allocate the quantization bits $B_j$ to each channel such that $B_0 \geq B_1 \geq \cdots \geq B_{M-1}$. In essence, more bits and greater resolution are allocated to the channels with greater signal energy. Observe that the objective function $\eta$ can be rewritten as

$$\eta = \sum_{j=0}^{M-2} \left(2^{-B_j} - 2^{-B_{j+1}}\right)\left(\sum_{k=0}^{j} {\sigma_k}^2\right) + 2^{-B_{M-1}}\left(\sum_{k=0}^{M-1} {\sigma_k}^2\right). \quad (53)$$

The last term is constant for all filter banks and can be ignored. Since

$$2^{-B_j} - 2^{-B_{j+1}} \leq 0, \quad (54)$$

$\eta$ is minimized by a PCFB, which by the majorization property maximizes all the partial sums

$$\sum_{k=0}^{j} {\sigma_k}^2 \quad (55)$$

for $j = 0, 1, \ldots, M-2$. ■

### B. Minimum Mean Square Error Filter Bank Approximation

The band partitioning strategy proposed in this paper is to design a filter bank approximation to the ideal PCFB which is adapted to the spectrum of a particular transmit signal. To begin, the polyphase matrix of the desired PCFB must be computed. Given a scalar transmit signal $x[n]$ and the corresponding $M$-fold blocked vector process $\mathbf{x}[n]$, let $\mathbf{D}(e^{j\omega})$ diagonalize the power spectral density matrix $\mathbf{S}_{xx}(e^{j\omega})$ of $\mathbf{x}[n]$ for each $\omega$; that is

$$\mathbf{D}(e^{j\omega})\mathbf{S}_{xx}(e^{j\omega})\mathbf{D}^{\mathbf{H}}(e^{j\omega}) = \boldsymbol{\Lambda}(e^{j\omega}) \quad (56)$$

where $\boldsymbol{\Lambda}(e^{j\omega})$ is a diagonal matrix for all $\omega$ with diagonal entries equal to $[\lambda_0(e^{j\omega}), \lambda_1(e^{j\omega}), \ldots, \lambda_{M-1}(e^{j\omega})]^{\mathbf{T}} = \boldsymbol{\lambda}$ in order of descending magnitude. The polyphase matrix $\mathbf{D}(e^{j\omega})$ constructed by performing an eigendecomposition to diagonalize $\mathbf{S}_{xx}(e^{j\omega})$ and then setting $\mathbf{D}(e^{j\omega})$ equal to the unitary matrix of eigenvectors corresponding to the eigenvalues in descending order at each $\omega$ is the desired polyphase matrix of the ideal PCFB [21]. $\mathbf{D}(e^{j\omega})$ represents an unrealizable filter bank of infinite order within the class $\mathcal{C}$ of paraunitary filter banks. The class $\mathcal{C}$ may be thought of as the set of all $M \times M$ polynomial matrices $\mathbf{H}(e^{j\omega})$ that are unitary for all $\omega$. Recall that for causal and stable systems this condition also implies (27). An algorithm for approximating the unrealizable filter bank $\mathbf{D}(e^{j\omega})$ using a realizable FIR PUFB will be described in this section. The next section presents an algorithm for deriving a PRFB approximation.

Given $\mathbf{D}(e^{j\omega})$, a FIR PUFB approximation $\mathbf{H}(e^{j\omega})$ may be designed by minimizing the mean square error

$$\rho = \frac{1}{2\pi}\int_0^{2\pi} \left\|\mathbf{D}(e^{j\omega}) - \mathbf{H}(e^{j\omega})\right\|_2^2 d\omega. \quad (57)$$

To solve this problem using unconstrained minimization techniques the paraunitary condition may be embedded into the objective function by decomposing $\mathbf{H}(e^{j\omega})$. Specifically, any $M$-by-$M$ causal FIR paraunitary system with real filter coefficients may be written as (see [15, p. 729])

$$\mathbf{H}(e^{j\omega}) = \mathbf{R}_N \mathbf{\Lambda}(e^{j\omega}) \mathbf{R}_{N-1} \mathbf{\Lambda}(e^{j\omega}) \cdots \mathbf{\Lambda}(e^{j\omega}) \mathbf{R}_1, \quad (58)$$

where $N-1$ is equal to the McMillan degree of $\mathbf{H}(e^{j\omega})$, the $\mathbf{R}_j$ are orthogonal matrices, and $\mathbf{\Lambda}(e^{j\omega})$ is the degree-one delay chain matrix

$$\mathbf{\Lambda}(e^{j\omega}) = \begin{bmatrix} \mathbf{I} & \mathbf{0} \\ \mathbf{0} & e^{-j\omega} \end{bmatrix}. \quad (59)$$

The McMillan degree of a multi-input and multi-output causal system refers to the minimum number of delay units (i.e., $e^{-j\omega}$ elements) required to implement it. The $M$ filters described by (58) have length $MN$.

Using the decomposition in (58) a PUFB may be designed by writing each orthogonal matrix $\mathbf{R}_j$ as a product of Givens rotation matrices so that the control variables in the optimization problem become rotation angles. Any $M$-by-$M$ orthogonal matrix $\mathbf{R}_j$ can be decomposed into the product sequence of $\frac{1}{2}M(M-1)$ Givens rotation matrices $S_{kl}$ as in

$$\mathbf{R}_j = \{\mathbf{S}_{M-2,M-1}\} \cdots \{\mathbf{S}_{1,M-1} \cdots \mathbf{S}_{12}\} \{\mathbf{S}_{0,M-1} \cdots \mathbf{S}_{01}\}. \quad (60)$$

Each matrix $\mathbf{S}_{kl}$ parameterized by the $m$th rotation angle has a form

$$[\mathbf{S}_{kl}]_{ij} = \begin{cases} 1, & \text{for } i = j \neq k \text{ or } l; \\ \cos(\theta_m), & \text{for } i = j = k \text{ or } l; \\ -\sin(\theta_m), & \text{for } i = l \text{ and } j = k; \\ \sin(\theta_m), & \text{for } i = k \text{ and } j = l; \\ 0, & \text{otherwise} \end{cases} \quad (61)$$

where the row and column numbers are indexed starting from zero.

### C. Gradient Computation

The gradient vector of the objective function $\rho$ can be computed in a straightforward manner using the product rule. For example, if the orthogonal matrix $\mathbf{R}_k$ depends on the parameter $\theta_m$ through the factor $\mathbf{S}_{pq}(\theta_m)$, then

$$\frac{\partial \rho}{\partial \theta_m} = \frac{-1}{2\pi} \int_0^{2\pi} 2Re\left\{\mathrm{tr}\left[\mathbf{V}_m(\boldsymbol{\theta}, \omega)\right]\right\} d\omega \quad (62)$$

where

$$\mathbf{V}_m(\boldsymbol{\theta}, \omega) = \mathbf{D}^{\mathbf{H}}(e^{j\omega}) \mathbf{R}_N \mathbf{\Lambda}(e^{j\omega}) \cdots \frac{\partial \mathbf{R}_k}{\partial \theta_m} \mathbf{\Lambda}(e^{j\omega}) \cdots \mathbf{\Lambda}(e^{j\omega}) \mathbf{R}_1 \quad (63)$$

and

$$\frac{\partial \mathbf{R}_k}{\partial \theta_m} = \mathbf{S}_{M-2,M-1} \cdots \frac{\partial \mathbf{S}_{pq}(\theta_m)}{\partial \theta_m} \cdots \mathbf{S}_{0,M-1} \ldots \mathbf{S}_{01}. \quad (64)$$

The entries of the matrix $\partial \mathbf{S}_{pq}(\theta_m)/\partial \theta_m$ are equal to

$$\left[\frac{\partial \mathbf{S}_{pq}(\theta_m)}{\partial \theta_m}\right]_{ij} = \begin{cases} \cos(\theta_m), & \text{for } i = p \text{ and } j = q; \\ -\cos(\theta_m), & \text{for } i = q \text{ and } j = p; \\ -\sin(\theta_m), & \text{for } i = j = p \text{ or } q; \\ 0, & \text{otherwise.} \end{cases} \quad (65)$$

Once the gradient vector is computed, an optimization routine similar to the conjugate gradient algorithm described in Section II, Algorithm 1 can be used to find a local optimum. The number of free parameters for a PUFB with McMillan degree $N-1$ would be $\frac{1}{2}NM(M-1)$. Since the objective function is not convex the algorithm may converge to a local optimum which depends somewhat on the initial values of the rotation angles. Furthermore, since the phase of the eigenvectors which comprise the desired PCFB polyphase matrix is ambiguous, a phase feedback technique described in [22] should also be employed to further improve approximation performance.

### D. Global vs Local Optimum

The PCFB design algorithms proposed in this paper do not guarantee a globally optimal solution. The problem of designing globally optimal PCFBs has been previously studied in the literature and two well known algorithms are presented by Moulin [23] and Tuqan [24]. Moulin proposes calculating an energy compaction filter for the first filter bank channel and then completing the rest of the filter bank via an appropriate covariance matrix eigendecomposition. The desired energy compaction filter is obtained by spectral factorization of an optimized product filter $P_0(z)$ which is the local (and global) solution to a linear semi-infinite programming problem. The compaction filter is nonunique since each of the spectral factors of $P_0(z)$ correspond to a global maximum of the energy compaction function.

Tuqan derives a state-space description of the product filter corresponding to an energy compaction filter. The globally optimal product filter is calculated using a semi-definite programming method. An energy compaction filter is obtained from the globally optimal product filter after a spectral factorization step and will not be unique in terms of its spectral factors. Different compaction filter spectral factors will lead to varying filter banks with different performances [25], [26]. To arrive at the filter bank with the best performance, an exhaustive search of all the compaction filter spectral factors is necessary and each resulting filter bank must be evaluated independently. This process becomes exponentially computationally expensive with respect to the order of the compaction filter.

### E. No-Gain Scenarios

For general input power spectra and an arbitrary number of channels $M > 2$, PCFBs are known to exist only for two special classes of filter banks [26]. The first is the class of all transform coders in which the synthesis polyphase matrix is a constant unitary matrix. The second is the class of all infinite order PUFBs. If the PCFB exists for a particular filter bank class, then it is optimal for energy compaction. However, there are certain types of input power spectra for which the maximum compaction gain will be unity. Compaction gain is defined as the ratio of the peak

subband variance to the total input signal variance. Specifically, if the zero-mean WSS input process has a power spectral density of the form $S_{xx}(e^{j\omega}) = S_{xx}(e^{j\omega M})$ then all the decimated subband signals have identical power spectra and the maximum compaction gain is unity [20]. In this case, there will be no improvement in transmit nulling performance in the presence of quantization errors with a PCFB. Similarly, if the locally optimal FIR approximation to an ideal PCFB results in a partition of the frequency spectrum into $M$ uniform regions of width $2\pi/M$, then there will be no improvement in quantization performance as compared to a filter bank such as the DFTFB.

## VI. PRFB Approximation to Ideal PCFB

There is no requirement to restrict the filter bank approximations of ideal PCFBs solely to the class of PUFBs. A more general class of filter banks available to the designer which includes PUFBs as a special case is the class of PRFBs. By increasing the optimization search space to include PRFBs it may be possible to find a realizable PCFB approximation with lower errors or better performance. The proposed approach for deriving a parameterized representation of PRFBs suitable for numerical optimization is to find a decomposition of the paraunitary building block $\mathbf{R}_j(\boldsymbol{\theta})\boldsymbol{\Lambda}(z)$ equal to the form $\mathbf{P}(z;\boldsymbol{\theta})\mathbf{R}(z;\boldsymbol{\theta})\mathbf{P}(z;\boldsymbol{\theta})^{-1}$. One such decomposition which exists for any matrix over a field is the rational canonical form decomposition. If this decomposition exists for polyphase matrices, a building block for PRFBs may be derived by parameterizing the change of basis matrix $\mathbf{P}(z;\boldsymbol{\theta})$ and the rational canonical form matrix $\mathbf{R}(z;\boldsymbol{\theta})$ independently; as in $\mathbf{P}(z;\boldsymbol{\theta}_1)\mathbf{R}(z;\boldsymbol{\theta}_2)\mathbf{P}(z;\boldsymbol{\theta}_1)^{-1}$.

### A. Rational Canonical Form of Arbitrary Polyphase Matrices

*Definition:* Any $M$-by-$M$ matrix $\mathbf{A}$ over a field $F$ is similar to a unique matrix $\mathbf{R}$ in rational canonical form [27]. More precisely, there is an invertible $M$-by-$M$ matrix $\mathbf{P}$ over $F$ such that $\mathbf{P}^{-1}\mathbf{A}\mathbf{P} = \mathbf{R}$ is a block diagonal matrix whose diagonal blocks are the companion matrices for monic polynomials $a_1(x), a_2(x), \ldots, a_m(x)$ of degree at least one with $a_1(x)|a_2(x)|\ldots|a_m(x)$. The polynomials $a_i(x)$ are called the invariant factors of $\mathbf{A}$. The invariant factors are made unique by stipulating that they be monic. The product of the invariant factors of $\mathbf{A}$ is equal to the characteristic polynomial $c(x)$ of $\mathbf{A}$. The companion matrix $\mathbf{C}_{a(x)}$ associated with the monic polynomial $a(x) = x^K + b_{K-1}x^{K-1} + \cdots + b_1 x + b_0$ is the $K$-by-$K$ matrix with 1's down the first subdiagonal, $-b_0, -b_1, \ldots, -b_{K-1}$ down the last column, and zeros elsewhere,

$$\mathbf{C}_{a(x)} = \begin{bmatrix} 0 & 0 & \ldots & \ldots & \ldots & -b_0 \\ 1 & 0 & \ldots & \ldots & \ldots & -b_1 \\ 0 & 1 & \ldots & \ldots & \ldots & -b_2 \\ 0 & 0 & \ddots & & & \vdots \\ \vdots & \vdots & & \ddots & & \vdots \\ 0 & 0 & \ldots & \ldots & 1 & -b_{K-1} \end{bmatrix}. \quad (66)$$

For an arbitrary polyphase matrix $\mathbf{H}(z)$ in the ring $\mathbf{M}(N, C[z, z^{-1}])$, the characteristic polynomial is a polynomial in the indeterminate $x$ with coefficients from the Laurent polynomial ring $C[z, z^{-1}]$; i.e., $c(x) = \det[x\mathbf{I} - \mathbf{H}(z)]$ [28], [29]. The rational canonical form of $\mathbf{H}(z)$ is guaranteed to exist as a matrix over the field $K$ of rational functions (see [29, p. 477–8]). The elements in $K$ are functions of the form $p(z)/q(z)$; $q(z) \neq 0$ with the coefficients of $p(z)$ and $q(z)$ equal to scalars in $C$. The field $K$ is the smallest field containing the entries of $\mathbf{H}(z)$. The following claim shows that none of the entries in the rational canonical form matrix of $\mathbf{H}(z)$ are rational functions (which have an infinite impulse response) and in fact that the rational canonical form matrix is itself a FIR polyphase matrix also in the ring $\mathbf{M}(N, C[z, z^{-1}])$. The proof relies on Gauss's Lemma (stated in [29]) to show that the invariant factors of $\mathbf{H}(z)$ are Laurent polynomials.

*1) Claim 2:* The rational canonical form of the polyphase matrix $\mathbf{H}(z)$ is a matrix in the ring $\mathbf{M}(N, C[z, z^{-1}])$.

*Proof:* Since $C$ is a field, the ring $C[z, z^{-1}]$ is a Unique Factorization Domain. The field $K$ of rational functions is the field of fractions of $C[z, z^{-1}]$. The characteristic polynomial $c(x)$ of $\mathbf{H}(z)$ is in the ring $C[z, z^{-1}][x]$ and is reducible in $K[x]$. By Gauss's Lemma, if $c(x)$ can be factored in $K[x]$, then it is reducible in $C[z, z^{-1}][x]$. Consequently, the invariant factors of $\mathbf{H}(z)$ are polynomials in the ring $C[z, z^{-1}]$ and the rational canonical form is a matrix in the ring $\mathbf{M}(N, C[z, z^{-1}])$. ■

### B. Computation of Rational Canonical Form for Polyphase Matrices

In this section, a systematic procedure is presented for computing the rational canonical form of an arbitrary polyphase matrix. To compute the rational canonical form of the $M$-by-$M$ matrix $\mathbf{H}(z)$, one approach is to diagonalize the matrix $x\mathbf{I} - \mathbf{H}(z)$ [29]. Then the invariant factors of $\mathbf{H}(z)$ will appear on the diagonal. The direct sum of the companion matrices associated with each invariant factor yields the matrix $\mathbf{R}(z)$ in rational canonical form. By keeping track of the row operations used to diagonalize $x\mathbf{I} - \mathbf{H}(z)$, one can also construct the change of basis matrix $\mathbf{P}(z)$ such that $\mathbf{P}(z)^{-1}\mathbf{H}(z)\mathbf{P}(z) = \mathbf{R}(z)$.

The following three elementary row and column operations can be used to diagonalize $x\mathbf{I} - \mathbf{H}(z)$;

1) interchange two rows or columns,
2) add a multiple in the ring $K[x]$ of one row or column to another, e.g., add $p(x)$ times the $j$th row to the $i$th row,
3) multiply any row or column by a unit in $K[x]$, i.e., by a nonzero element in $K$.

The matrix $\mathbf{P}(z)$ can be computed systematically using the following procedure [29]. Let $d_1, \ldots, d_m$ denote the degrees of the monic nonconstant polynomials $a_1(x), \ldots, a_m(x)$ appearing on the diagonal. Start with a matrix $\mathbf{S} = \mathbf{I}$, the identity matrix. For each row operation used to diagonalize $x\mathbf{I} - \mathbf{H}(z)$, change the matrix $\mathbf{S}$ as follows;

1) if the $i$th and $j$th rows were interchanged, then interchange the $i$th and $j$th columns of $\mathbf{S}$,
2) if $Row_i + p(x)Row_j \rightarrow Row_i$ then subtract the product of the matrix $p(\mathbf{H}(z))$ times the $i$th column of $\mathbf{S}$ from the $j$th column of $\mathbf{S}$, i.e., $Col_j - p(\mathbf{H}(z))Col_i \rightarrow Col_j$,
3) if the $j$th row is multiplied by a unit $u$, then divide the $j$th column of $\mathbf{S}$ by $u$.

Once the matrix $x\mathbf{I} - \mathbf{H}(z)$ has been diagonalized, the first $M - m$ columns of $\mathbf{S}$ will be zero. Then for each $i = 1, \ldots, m$ multiply the $i$th nonzero column of $\mathbf{S}$ successively by $\mathbf{H}(z)^0 = \mathbf{I}, \mathbf{H}(z), \mathbf{H}(z)^2, \ldots, \mathbf{H}(z)^{d_i - 1}$, where $d_i$ is the degree of $a_i(x)$. Use the resulting column vectors in

TABLE I
COMPUTATION OF RATIONAL CANONICAL FORM

| Steps to Compute $\mathbf{R}(z)$ | Steps to Compute $\mathbf{P}(z)$ |
|---|---|
| **Step 1**: Form the matrix $x\mathbf{I}-\mathbf{H}(z)$ | **Step 1**: Form the matrix $\mathbf{S}=\mathbf{I}$ |
| **Step 2**: $-\sin(\theta)R_1 \rightarrow R_1$; $(x-\cos(\theta))R_2 \rightarrow R_2$ | **Step 2**: $-(1/\sin(\theta))C_1 \rightarrow C_1$; $[\mathbf{H}(z)-\cos(\theta)\mathbf{I}]C_1+C_2 \rightarrow C_1$ |
| **Step 3**: $-R_1+R_2 \rightarrow R_2$ | **Step 3**: $\sin(\theta)C_1 \rightarrow C_1$ |
| **Step 4**: $(1/\sin(\theta))R_1 \rightarrow R_1$ | **Step 4**: $(z/\sin(\theta))C_2 \rightarrow C_2$; $-C_1 \rightarrow C_1$ |
| **Step 5**: $z^{-1}\sin(\theta)R_2 \rightarrow R_2$; $(x^2-x\cos(\theta)(1+z^{-1})+z^{-1})R_1 \rightarrow R_1$ | **Step 5**: $C_1-(\mathbf{H}(z)^2-\cos(\theta)\mathbf{H}(z)(1+z^{-1})+z^{-1}\mathbf{I})C_2 \rightarrow C_2$ |
| **Step 6**: $-R_1 \rightarrow R_1$ | **Step 6**: $[\mathbf{H}(z)-\cos(\theta)\mathbf{I}]C_1 \rightarrow C_1$; $\sin(\theta)z^{-1}C_2 \rightarrow C_2$ |
| **Step 7**: $R_1+R_2 \rightarrow R_1$ | **Step 7**: $[\mathbf{H}(z)^2-\cos(\theta)\mathbf{H}(z)(1+z^{-1})+z^{-1}\mathbf{I}]C_1 \rightarrow C_1$ |
| **Step 8**: $[1/(x-\cos(\theta))]R_1 \rightarrow R_1$; $[1/(z^{-1}\sin(\theta))]R_2 \rightarrow R_2$ | **Step 8**: Now, $\mathbf{S}=\begin{bmatrix}0 & 0\\ 0 & -2z^{-1}\sin(\theta)^2\end{bmatrix}$ Also, $m=1, d_1=2$ |
| **Step 9**: $[1/(x^2-x\cos(\theta)(1+z^{-1})+z^{-1})]R_1 \rightarrow R_1$ | **Step 9**: Form the matrix, $\mathbf{P}(z)=\begin{bmatrix}\mathbf{I}C_2 & \mathbf{H}(z)C_2\end{bmatrix}$ |

this order as the next $d_i$ columns of a matrix $\mathbf{P}(z)$. Then $\mathbf{P}(z)^{-1}\mathbf{H}(z)\mathbf{P}(z)=\mathbf{R}(z)$.

### C. Parameterized Representation of PRFBs

Set $\mathbf{H}(z;\theta)$ equal to the 2-by-2 paraunitary building block taken from (58)

$$\mathbf{H}(z;\theta)=\begin{bmatrix}\cos\theta & \sin\theta\\ -\sin\theta & \cos\theta\end{bmatrix}\begin{bmatrix}1 & 0\\ 0 & z^{-1}\end{bmatrix}. \tag{67}$$

By applying the steps listed in Table I to compute the rational canonical form $\mathbf{R}(z)$ of $\mathbf{H}(z)$ and the change of basis matrix $\mathbf{P}(z)$, one obtains

$$\mathbf{R}(z;\theta)=\begin{bmatrix}0 & -z^{-1}\\ 1 & \cos\theta(1+z^{-1})\end{bmatrix} \tag{68}$$

and

$$\mathbf{P}(z;\theta)=-2(\sin\theta)^2z^{-1}\begin{bmatrix}0 & z^{-1}\sin\theta\\ 1 & z^{-1}\cos\theta\end{bmatrix} \tag{69}$$

with

$$\mathbf{P}(z;\theta)^{-1}=-\frac{1}{2}(\csc\theta)^2z\begin{bmatrix}-\cot\theta & 1\\ z\csc\theta & 0\end{bmatrix}. \tag{70}$$

As desired $\mathbf{P}(z;\theta)^{-1}\mathbf{H}(z;\theta)\mathbf{P}(z;\theta)=\mathbf{R}(z;\theta)$. Also, $\mathbf{R}(z;\theta)$ is invertible since $\mathbf{H}(z;\theta)$ is invertible.

A building block for PRFBs may be constructed from the rational canonical form decomposition of the paraunitary building block $\mathbf{H}(z;\theta)$ by parameterizing the matrix $\mathbf{R}(z;\theta)$ and the conjugation matrices $\mathbf{P}(z;\theta)$ and $\mathbf{P}(z;\theta)^{-1}$ independently. The result after rearranging terms is

$$\mathbf{G}(z;\theta_1,\theta_2)=\begin{bmatrix}0 & \sin\theta_1\\ 1 & \cos\theta_1\end{bmatrix}\begin{bmatrix}0 & -1\\ 1 & 2\cos\theta_2\end{bmatrix}\times\begin{bmatrix}-\cos\theta_1 & \sin\theta_1\\ 1 & 0\end{bmatrix}\begin{bmatrix}1 & 0\\ 0 & z^{-1}\end{bmatrix}\csc\theta_1. \tag{71}$$

A PRFB satisfies the property that $\mathbf{G}(z)\mathbf{E}(z)=cz^{-m}\mathbf{I}$, where $\mathbf{G}(z)$ is the analysis polyphase matrix and $\mathbf{E}(z)$ is the synthesis polyphase matrix, with $c\neq 0$ and $m$ an integer. Thus the system with analysis polyphase matrix $\mathbf{G}(z;\theta_1,\theta_2)$ and synthesis polyphase matrix $\mathbf{E}(z;\theta_1,\theta_2)$ equal to

$$\mathbf{E}(z;\theta_1,\theta_2)=\begin{bmatrix}1 & 0\\ 0 & z\end{bmatrix}\begin{bmatrix}0 & \sin\theta_1\\ 1 & \cos\theta_1\end{bmatrix}\begin{bmatrix}2\cos\theta_2 & 1\\ -1 & 0\end{bmatrix}\times\begin{bmatrix}-\cos\theta_1 & \sin\theta_1\\ 1 & 0\end{bmatrix}\csc\theta_1 \tag{72}$$

is perfect reconstruction since $\mathbf{E}(z;\theta_1,\theta_2)=\mathbf{G}(z;\theta_1,\theta_2)^{-1}$. Notice that for the special case when $\theta_1=\theta_2$, $\mathbf{G}(z;\theta)$ is paraunitary. Therefore, the set of PRFBs constructed using this decomposition includes the set of all PUFBs as a proper subset. However, there may exist PRFBs which cannot be represented in the form (71) and (72) so this factorization of PRFBs is not necessarily complete. The number of free parameters for a PRFB with McMillan degree $N-1$ would be no more than $NM(M-1)$.

## VII. APPLICATION TO PCFB APPROXIMATION

It is possible to accurately approximate an ideal PCFB by searching over the space of PRFBs which includes the set of all PUFBs as a subset. The objective function is similar to (57), with $\mathbf{H}(e^{j\omega})$ set equal to the parameterized decomposition of a PRFB. The solution can be found using gradient descent nonlinear minimization techniques. Using the perfect reconstruction building block proposed in (71), the $M$-by-$M$ analysis polyphase matrix of a PRFB may be written as

$$\mathbf{G}(e^{j\omega})=\mathbf{T}_N\mathbf{\Lambda}(e^{j\omega})\mathbf{T}_{N-1}\mathbf{\Lambda}(e^{j\omega})\cdots\mathbf{\Lambda}(e^{j\omega})\mathbf{T}_1, \tag{73}$$

where $N-1$ is equal to the McMillan degree of $\mathbf{G}(e^{j\omega})$ and $\mathbf{\Lambda}(e^{j\omega})$ is the degree-one delay chain matrix. The matrices $\mathbf{T}_j$ are equal to

$$\mathbf{T}_j=\{\mathbf{P}_{M-2,M-1}\}\cdots\{\mathbf{P}_{1,M-1}\cdots\mathbf{P}_{12}\}\{\mathbf{P}_{0,M-1}\cdots\mathbf{P}_{01}\} \tag{74}$$

where

$$\mathbf{P}_{kl}(\theta_m,\theta_{m+1})=\mathbf{U}_{kl}(\theta_m)\mathbf{V}_{kl}(\theta_{m+1})\mathbf{W}_{kl}(\theta_m) \tag{75}$$

with

$$[\mathbf{U}_{kl}]_{ij}=\begin{cases}1, & \text{for } i=j\neq k \text{ or } l;\\ 0, & \text{for } i=j=k;\\ \cos(\theta_m), & \text{for } i=j=l;\\ 1, & \text{for } i=l \text{ and } j=k;\\ \sin(\theta_m), & \text{for } i=k \text{ and } j=l;\\ 0, & \text{otherwise.}\end{cases} \tag{76}$$

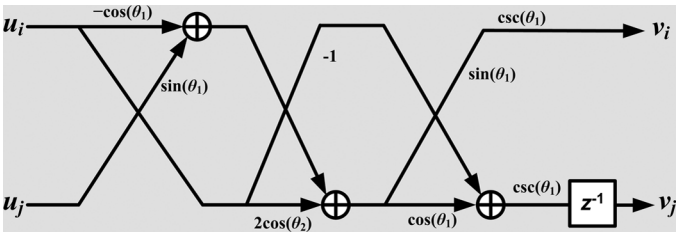


Fig. 5. PRFB lattice structure.

$$[\mathbf{V}_{kl}]_{ij} = \begin{cases} 1, & \text{for } i = j \neq k \text{ or } l; \\ 0, & \text{for } i = j = k; \\ 2\cos(\theta_{m+1}), & \text{for } i = j = l; \\ 1, & \text{for } i = l \text{ and } j = k; \\ -1, & \text{for } i = k \text{ and } j = l; \\ 0, & \text{otherwise.} \end{cases} \quad (77)$$

$$[\mathbf{W}_{kl}]_{ij} = \begin{cases} 1, & \text{for } i = j \neq k \text{ or } l; \\ -\cos(\theta_m), & \text{for } i = j = k; \\ 0, & \text{for } i = j = l; \\ 1, & \text{for } i = l \text{ and } j = k; \\ \sin(\theta_m), & \text{for } i = k \text{ and } j = l; \\ 0, & \text{otherwise.} \end{cases} \quad (78)$$

The synthesis polyphase matrix is

$$\mathbf{E}(e^{j\omega}) = \mathbf{B}_1\mathbf{\Lambda}(e^{j\omega})^{\mathbf{H}}\mathbf{B}_2\mathbf{\Lambda}(e^{j\omega})^{\mathbf{H}} \cdots \mathbf{\Lambda}(e^{j\omega})^{\mathbf{H}}\mathbf{B}_N, \quad (79)$$

where

$$\mathbf{B}_j = \{\mathbf{C}_{M-2,M-1}\} \cdots \{\mathbf{C}_{1,M-1} \cdots \mathbf{C}_{12}\} \{\mathbf{C}_{0,M-1} \cdots \mathbf{C}_{01}\} \quad (80)$$

and

$$\mathbf{C}_{kl}(\theta_m, \theta_{m+1}) = \mathbf{U}_{kl}(\theta_m)\mathbf{X}_{kl}(\theta_{m+1})\mathbf{W}_{kl}(\theta_m) \quad (81)$$

with

$$[\mathbf{X}_{kl}]_{ij} = \begin{cases} 1, & \text{for } i = j \neq k \text{ or } l; \\ 2\cos(\theta_{m+1}), & \text{for } i = j = k; \\ 0, & \text{for } i = j = l; \\ -1, & \text{for } i = l \text{ and } j = k; \\ 1, & \text{for } i = k \text{ and } j = l; \\ 0, & \text{otherwise.} \end{cases} \quad (82)$$

### A. Overall Implementation Complexity

The primary advantage of the band partitioned array architecture is that the filter banks allow TDL processing to be performed within the subbands at a sampling rate $M$ times lower than the non-band partitioned array. The TDL coefficients in each subband are determined once for any combination of null and main beam pointing directions. Once computed, the TDL coefficients are stored and retrieved from digital memory as needed. The computational throughput required for TDL processing at each array element is the same with or without band partitioning (since an $M$-channel filterbank performs $M$ times more TDL operations but at a rate $M$ times slower).

The design complexity of a PUFB or a PRFB is a computational cost also incurred once for a given input signal. A PRFB will require more computations than a PUFB to implement as the lattice structure corresponding to (71) and shown in Fig. 5 indicates. The input signals are $u_i$ in the $i$th channel and $u_j$ in the $j$th channel. The corresponding output signals are $v_i$ and $v_j$. Define a flop to be one floating point operation, either multiplication or addition. The real scalars shown on the branches of the lattice diagram are precomputed and multiply the incoming signal values. Negation does not count as a flop. Counting the number of operations shown in the lattice diagram reveals that the PRFB lattice requires 7 multiplies and 3 adds, or 10 flops. A similar comparison to the lattice structure of a PUFB shows that a PUFB building block requires 4 multiplies and 2 adds, or 6 flops [15]. Thus the PRFB entails 67% more computations than a PUFB. The total number of flops required to implement the analysis and synthesis sections of an $M$-channel PRFB with McMillan degree $N-1$ is $10NM(M-1)$ per output sample. An $M$-channel PUFB with McMillan degree $N-1$ requires $6NM(M-1)$ flops per output sample. These filter bank computations incur an additional latency compared to the TDL array architecture of Fig. 3 but do not otherwise affect array performance.

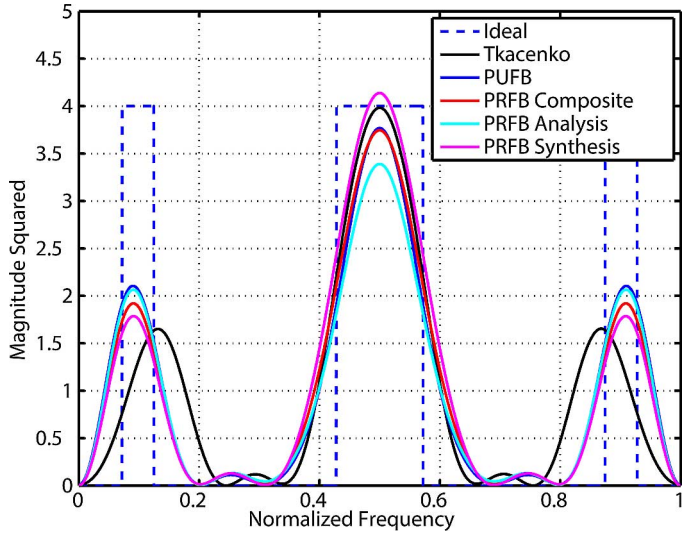


Fig. 6. Filter 1—Ideal, PUFB, PRFB, Tkacenko.

## VIII. Filter Bank Design Results

Using the proposed parameterized decomposition for PRFBs and a conjugate gradient algorithm to minimize the MSE in (57), a PRFB approximation to an ideal brickwall PCFB was derived for $M = 4$ and McMillan degree $N = 1$. The length of the channel filters is 8 taps. The results are plotted in Fig. 6 for the first frequency subband which shows the magnitude squared response of the PRFB analysis filters $\left|H_0(e^{j\omega})\right|^2$, synthesis filters $\left|F_0(e^{j\omega})\right|^2$, and their composite response $\left|H_0(e^{j\omega})F_0(e^{j\omega})\right|$. Also shown are the PUFB analysis filters constructed using the Givens decomposition as well as a PUFB approximation with the same McMillan degree designed using the recent algorithm by Tkacenko [22]. The results show a close approximation of the PRFB and PUFB channel filters to the ideal PCFB brickwall filters. The perfect reconstruction polyphase matrix is parameterized by 24 rotation angles and the paraunitary polyphase matrix is parameterized by 12 rotation angles.

TABLE II
ERROR METRICS FOR PCFB APPROXIMATIONS

| Overall Metric | PUFB | PRFB | Tkacenko |
|---|---|---|---|
| $\rho$ (57) | **1.5582** | 1.5597 | 1.7022 |
| $\max_j L_\infty^{(j)}$ | **1.5589** | $A$ 1.5618<br>$S$ 1.5803<br>$C$ 1.5710 | 1.7370 |
| $\sum_j L_2^{(j)}$ | 1.5575 | $A$ **1.5353**<br>$S$ 1.6438<br>$C$ 1.5662 | 1.7017 |
| **Filter Metric** | **PUFB** | **PRFB** | **Tkacenko** |
| $L_\infty^{(1)}$ | 1.3809 | $A$ **1.3650**<br>$S$ 1.5560<br>$C$ 1.4463 | 1.4816 |
| $L_2^{(1)}$ | **0.4070** | $A$ 0.4167<br>$S$ 0.4382<br>$C$ 0.4232 | 0.4741 |
| $L_\infty^{(2)}$ | **1.3529** | $A$ 1.4180<br>$S$ 1.4653<br>$C$ 1.4211 | 1.7370 |
| $L_2^{(2)}$ | 0.5103 | $A$ **0.4690**<br>$S$ 0.5597<br>$C$ 0.5054 | 0.5239 |
| $L_\infty^{(3)}$ | 1.5589 | $A$ 1.5618<br>$S$ 1.5803<br>$C$ 1.5710 | **1.4105** |
| $L_2^{(3)}$ | 0.3971 | $A$ **0.3907**<br>$S$ 0.4009<br>$C$ 0.3937 | 0.4268 |
| $L_\infty^{(4)}$ | 1.3731 | $A$ 1.4592<br>$S$ **1.3033**<br>$C$ 1.3689 | 1.4098 |
| $L_2^{(4)}$ | **0.2431** | $A$ 0.2589<br>$S$ 0.2450<br>$C$ 0.2439 | 0.2769 |

Table II details the approximation performance for the magnitude response in each filter bank channel. The error metric $L_\infty^{(j)} = \max_\omega \left| |H_j(e^{j\omega})| - D_j(e^{j\omega}) \right|$ where $D_j(e^{j\omega})$ is the brickwall response of the ideal PCFB filter in the $j$th subband. The error metric $L_2^{(j)} = \frac{1}{2\pi}\int_0^{2\pi} \left| |H_j(e^{j\omega})| - D_j(e^{j\omega}) \right|^2 d\omega$. For the case of the PRFB, the error metrics are shown separately for each analysis filter $H_j(e^{j\omega})$ (denoted by $A$), synthesis filter $F_j(e^{j\omega})$ (denoted by $S$) and their composite response $H_j(e^{j\omega})F_j(e^{j\omega})$ (denoted by $C$).

Fig. 7 illustrates the majorization property for the FIR approximations to the ideal PCFB. A real autoregressive process was assumed for the input signal with poles at $p_0 = 0.95e^{j0.2\pi}$, $p_1 = 0.8e^{j0.9\pi}$, $\overline{p}_0$, and $\overline{p}_1$. The plot overlays the cumulative sum of subband variances (51), expressed as percentages of the total input signal energy, for the PUFB, DFTFB, Tkacenko filter bank and the ideal PCFB. For the PRFB, the cumulative sum of subband cross-covariances is shown which was obtained by replacing $\mathbf{H}^{\mathbf{H}}(e^{j\omega})$ in (51) with the synthesis polyphase matrix $\mathbf{E}^{\mathbf{H}}(e^{j\omega})$. Fig. 7 confirms that the FIR PCFB approximations pack more signal energy into the lower subbands than the DFTFB.

## IX. WIDEBAND TRANSMIT NULLING RESULTS

### A. In the Absence of Quantization Errors

Fig. 8 illustrates the optimized transmit pattern for a point null at 19.57° over a fractional bandwidth of 40% for an ideal linear array of 32 elements with a DFTFB behind each array element and $M = 4$. Fractional bandwidth is defined as the transmitted signal bandwidth divided by the array center frequency. The TDL in each frequency subband has 3 tap coefficients represented as double precision floating point numbers. The average null depth over the entire signal bandwidth is $-96.0$ dBi as defined in (10). There is some minor ripple in the peak main beam gain as a function of frequency but otherwise only benign distortions appear in the main beam pattern. A PUFB array architecture yielded an average null depth of $-89.5$ dBi in the absence of coefficient quantization errors and the PRFB array architecture resulted in an average null depth of $-92.8$ dBi. An array architecture with ideal brickwall PCFB filters resulted in an average null depth of $-92.3$ dBi.

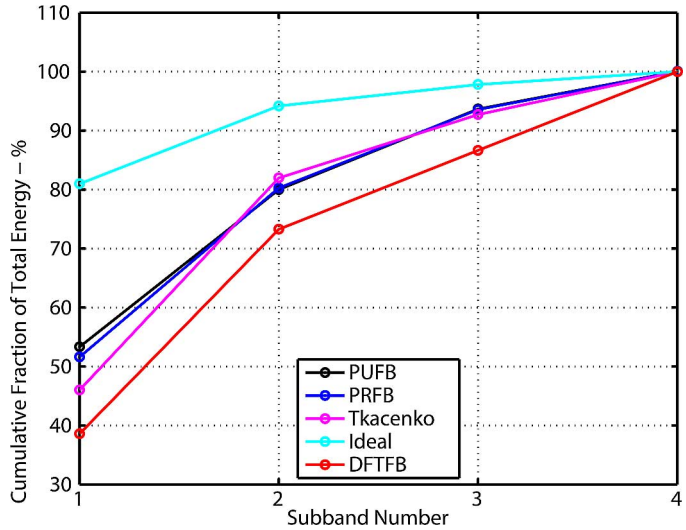


Fig. 7. Majorization property of approximated PCFB.

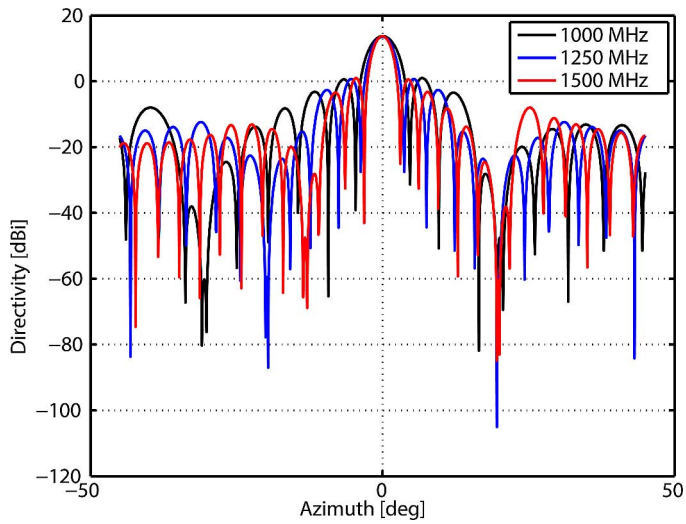


Fig. 8. Point null—DFTFB solution.

### B. In the Presence of Quantization Errors

To compare nulling performance for different filter bank schemes accurately in the presence of TDL quantization errors the chosen performance metric is the average ERP of the array over the signal bandwidth in the null direction $\theta_1$. This metric

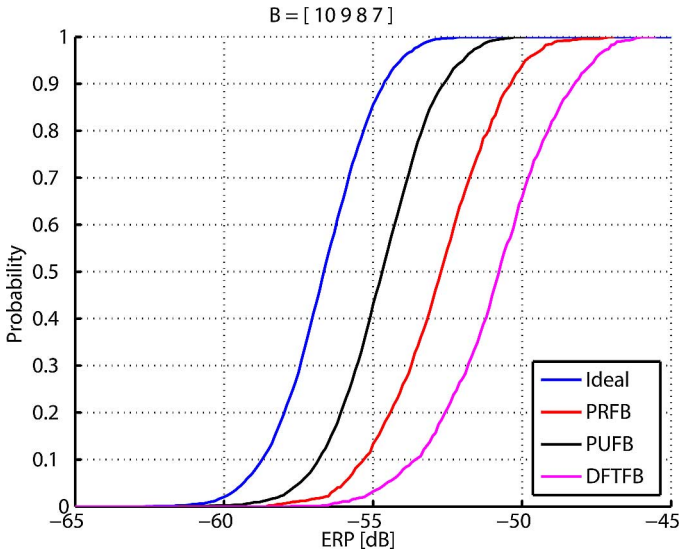


Fig. 9. Cumulative probability of ERP in null direction.

accounts for the cases where signal energy is not uniformly distributed over the instantaneous transmit bandwidth. Assuming an $N$-element linear array with isotropic elements, the average ERP over the signal bandwidth is computed as

$$ERP = \frac{1}{P}\sum_{i=0}^{P-1}\left|\sum_{n=0}^{N-1}\widehat{X}_n(e^{j\omega_i})e^{-j\left(\frac{\omega_i}{c}\right)Dn\sin\theta}\right|^2 \tag{83}$$

where $\widehat{X}_n(e^{j\omega})$ is the spectrum of the filter bank output behind the $n$th array element,

$$\widehat{X}_n(e^{j\omega}) = \sum_{l=0}^{M-1} A_{ln}(e^{j\omega})X\left(e^{j\left(\omega-\frac{2\pi l}{M}\right)}\right) \tag{84}$$

and

$$A_{ln}(e^{j\omega}) = \frac{1}{M}\sum_{k=0}^{M-1} H_k\left(e^{j\left(\omega-\frac{2\pi l}{M}\right)}\right)T_{kn}(e^{j\omega M})F_k(e^{j\omega}). \tag{85}$$

In the above equations $X(e^{j\omega})$ is the spectrum of the input signal to each filter bank, $T_{kn}(e^{j\omega})$ is the spectrum of the TDL in the $k$th subband of the $n$th array element, $H_k(e^{j\omega})$ is the frequency response of the $k$th analysis filter, $F_k(e^{j\omega})$ is the frequency response of the $k$th synthesis filter, $P$ is the number of frequency samples taken within the transmit signal bandwidth, and $D$, $\lambda$, $c$, $\theta$ are as defined in (2) and (4).

The nulling performance of each array architecture was determined by superimposing random quantization errors on the ideal TDL coefficients in each subband and computing the average ERP over the signal bandwidth as defined by (83) for 2048 frequency samples taken over a 40% fractional bandwidth for a linear array of 32 elements. The TDL coefficients were computed for each array architecture by maximizing (33) to yield a null at 19.57° with the main beam pointed at boresight. If $B_j$ denotes the number of bits allocated to the $j$th subband then the quantization errors applied to the $j$th TDL in each filter bank were uniformly distributed in the interval $[-q_j/2, q_j/2]$ with $q_j = L/2^{B_j}$ and $L$ as defined in (41). The variance of the quantization errors applied to each TDL coefficient in the $j$th subband of each filterbank is therefore $q_j^2/12; 0 \le j \le M-1$ [17]. Fig. 9 illustrates the cumulative distribution of ERP for all 3 FIR filterbanks and the ideal PCFB with brickwall filters for the bit allocation scheme $B_0 = 10, B_1 = 9, B_2 = 8, B_3 = 7$. This plot is typical for all the cases considered and shows that the FIR approximations to the ideal PCFB yielded the best nulling performance (i.e., lowest ERP in the null direction) as compared to the DFTFB.

TABLE III
ERP (dB) FOR DIFFERENT BIT ALLOCATION SCHEMES

| Bit Scheme | Ideal | PRFB | PUFB | DFTFB |
|---|---|---|---|---|
| 13,11,9,7 | −59.43 | −56.54 | **−57.26** | −53.01 |
| | −52.73 | −50.52 | **−51.68** | −46.83 |
| 12,10,9,7 | −59.14 | −56.02 | **−56.90** | −52.87 |
| | −52.05 | **−51.25** | −51.19 | −46.78 |
| 12,10,8,6 | −53.52 | −50.61 | **−51.24** | −47.01 |
| | −46.45 | **−45.21** | −44.79 | −40.43 |
| 10,9,8,7 | −56.33 | −52.34 | **−54.37** | −50.35 |
| | −51.42 | −46.94 | **−49.90** | −45.55 |
| 11,9,6,6 | −49.68 | −42.36 | **−46.47** | −40.20 |
| | −44.35 | −36.06 | **−39.00** | −34.36 |
| 11,9,7,5 | −47.51 | −44.40 | **−45.27** | −40.98 |
| | −39.35 | −39.05 | **−39.27** | −34.02 |
| 9,8,7,6 | −50.30 | −46.34 | **−48.27** | −44.32 |
| | −44.60 | −41.04 | **−43.55** | −38.32 |
| 10,8,6,5 | −46.11 | −41.05 | **−43.60** | −38.58 |
| | −40.6 | −35.96 | **−37.71** | −33.09 |
| 10,8,6,4 | −41.48 | −38.50 | **−39.30** | −34.99 |
| | −35.63 | **−32.65** | −31.73 | −28.92 |
| 7,7,6,6 | −42.89 | −40.45 | **−42.17** | −39.28 |
| | −36.93 | −34.91 | **−36.95** | −34.41 |
| 8,7,6,5 | −44.32 | −40.29 | **−42.30** | −38.33 |
| | −39.47 | −35.60 | **−37.72** | −32.93 |
| 8,6,5,4 | −39.25 | −34.51 | **−36.76** | −32.42 |
| | −35.08 | −29.58 | **−32.10** | −27.80 |
| 7,6,5,4 | −38.25 | −34.35 | **−36.24** | −32.32 |
| | −33.20 | −28.18 | **−31.89** | −26.88 |
| 7,5,5,4 | −36.64 | −32.57 | **−34.24** | −32.05 |
| | −32.67 | −28.60 | **−29.87** | −26.89 |
| 6,5,4,4 | −33.85 | −29.11 | **−32.02** | −27.63 |
| | −30.14 | −23.46 | **−27.28** | −22.26 |

One would expect that by partitioning the signal spectrum using an approximated PCFB and then assigning more quantization bits to the subbands with greater signal energy, the ERP in the null direction will be reduced. In fact, Monte Carlo results shown in Table III confirm this hypothesis. Each row in Table III shows the average ERP (top value) and the peak ERP (bottom) in dB for the null direction 19.57° computed using (83) for different bit allocation schemes $\{B_0, B_1, B_2, B_3\}$ over 1000 Monte Carlo iterations. Also listed as a bound on performance are the average and peak ERP values obtained using the ideal brickwall PCFB filters. In each row of the table the lowest ERP between the PUFB, PRFB, and the DFTFB is shown in bold type. Table III shows that for every bit allocation scheme considered, the numerically optimized PRFB or PUFB approximation to an ideal PCFB resulted in the lowest average and peak ERP at the null location as compared to a DFTFB.

## X. CONCLUSION

In this paper, a wideband transmit nulling approach robust to quantization errors was introduced. The proposed array architecture consists of a filter bank inserted behind each array

element that partitions the transmit signal into independent subbands. A numerical algorithm was derived for computing the optimal TDL weights in each subband such that a wideband spatial null is created in the antenna transmit pattern. If the coefficients of the TDLs are subject to quantization errors, a band partitioning scheme which approximates an ideal PCFB yields superior performance compared to more conventional filter banks, such as the DFTFB.

## REFERENCES


[1] D. Day, "Robust phase-only nulling for adaptive and non-adaptive phased arrays," in *Proc. 2007 Asilomar Conf. Signal, Syst., Comput.*, Monterey, CA, USA, Nov. 4–7, 2007, pp. 2173–2176.

[2] D. Day, "Fast phase-only pattern nulling for large phased array antennas," in *Proc. 2009 IEEE Radar Conf.*, Pasadena, CA, USA, May 4–8, 2009, pp. 1–4.

[3] E. Dufort, "Pattern synthesis based on adaptive array theory," *IEEE Trans. Antennas Propag.*, vol. 37, no. 8, pp. 1011–1018, Aug. 1989.

[4] H. Steyskal, "Simple method for pattern nulling by phase perturbation," *IEEE Trans. Antennas Propag.*, vol. 31, no. 1, pp. 163–166, Jan. 1983.

[5] H. Steyskal, "Synthesis of antenna patterns with prescribed nulls," *IEEE Trans. Antennas Propag.*, vol. 30, no. 2, pp. 273–279, Mar. 1982.

[6] S. T. Smith, "Optimum phase-only adaptive nulling," *IEEE Trans. Signal Proces.*, vol. 47, no. 7, pp. 1835–1843, Jul. 1999.

[7] Y. Zhao, W. Liu, and R. Langley, "Subband design of fixed wideband beamformers based on the least squares approach," *Elsevier J. Signal Process.*, vol. 91, no. 4, pp. 1060–1065, Apr. 2011.

[8] Y. Zhang, K. Yang, and M. Amin, "Adaptive array processing for multipath fading mitigation via exploitation of filter banks," *IEEE Trans. Antennas Propag.*, vol. 49, no. 4, pp. 505–516, Apr. 2001.

[9] R. T. Compton, "The relationship between tapped delay-line and FFT processing in adaptive arrays," *IEEE Trans. Antennas Propag.*, vol. 36, no. 1, pp. 15–26, Jan. 1988.

[10] F. C. Lin, J. P. Hansen, J. McConnell, and K. Gerlach, "Experimental Wideband Multi-Channel Cancellation Performance," in *Proc. 2005 IEEE Radar Conf.*, Arlington, VA, USA, May 9–12, 2005, pp. 675–679.

[11] S. Weiss, R. Stewart, M. Schabert, I. Proudler, and M. Hoffman, "An efficient scheme for broadband adaptive beamforming," in *Proc. 33rd Asilomar Conf. Signals, Syst., Comput.*, Pacific Grove, CA, USA, Oct. 24–27, 1999, pp. 496–500.

[12] P. Vouras and T. Tran, "Wideband adaptive beamforming using linear phase filterbanks," in *Proc. 40th Asilomar Conf. Signals, Syst., Comput.*, Pacific Grove, CA, USA, Oct. 29–Nov. 1, 2006, pp. 2295–2299.

[13] N. Ishii and R. Kohno, "Spatial and temporal equalization based on an adaptive tapped delay line array antenna," presented at the 5th IEEE Int. Symp. Wireless Netw.: Catching the Mobile Future, The Hague, The Netherlands, Sep. 18–23, 1994.

[14] G. B. Folland, *Real Analysis: Modern Techniques and their Applications*. New York, NY, USA: Wiley, 1999.

[15] P. P. Vaidyanathan, *Multirate Systems and Filter Banks*. Upper Saddle River, NJ, USA: Prentice-Hall, 1993.

[16] G. Strang and T. Nguyen, *Wavelets and Filter Banks*. Wellesley, MA, USA: Wellesley-Cambridge Press, 1997.

[17] B. Widrow and I. Kollar, *Quantization Noise: Roundoff Error in Digital Computation, Signal Processing, Control, and Communications*. Cambridge, U.K.: Cambridge Univ. Press, 2008.

[18] B. Porat, *A Course in Digital Signal Processing*. New York, NY, USA: Wiley, 1997.

[19] M. K. Tsatsanis and G. B. Giannakis, "Principal component filter banks for optimal multiresolution analysis," *IEEE Trans. Signal Process.*, vol. 43, no. 8, pp. 1766–1777, Aug. 1995.

[20] P. P. Vaidyanathan, "Theory of optimal orthonormal subband coders," *IEEE Trans. Signal Process.*, vol. 46, no. 6, pp. 1528–1543, Jun. 1998.

[21] S. Akkarakaran and P. P. Vaidyanathan, "Filterbank optimization with convex objectives and the optimality of principal component forms," *IEEE Trans. Signal Process.*, vol. 49, no. 1, pp. 100–114, Jan. 2001.

[22] A. Tkacenko and P. P. Vaidyanathan, "Iterative greedy algorithm for solving the FIR paraunitary approximation problem," *IEEE Trans. Signal Process.*, vol. 54, no. 1, pp. 146–160, Jan. 2006.

[23] P. Moulin and M. K. Mihcak, "Theory and design of signal-adapted FIR paraunitary filter banks," *IEEE Trans. Signal Process.*, vol. 46, no. 4, pp. 920–929, Apr. 1998.

[24] J. Tuqan and P. P. Vaidyanathan, "A state space approach to the design of globally optimal FIR energy compaction filters," *IEEE Trans. Signal Process.*, vol. 48, no. 10, pp. 2822–2838, Oct. 2000.

[25] A. Tkacenko and P. P. Vaidyanathan, "On the spectral factor ambiguity of FIR energy compaction filter banks," *IEEE Trans. Signal Process.*, vol. 54, no. 1, pp. 380–385, Jan. 2006.

[26] A. Kirac and P. P. Vaidyanathan, "On existence of FIR principal component filter banks," in *Proc. IEEE Conf. Acoust., Speech, Signal Process.*, Seattle, WA, USA, May 12–15, 1998, pp. 1329–1332.

[27] R. A. Horn and C. R. Johnson, *Matrix Analysis*. Cambridge, U.K.: Cambridge Univ. Press, 1985.

[28] S. Lang, *Algebra*, 3rd ed. New York, NY, USA: Springer, 2002.

[29] D. S. Dummit and R. M. Foote, *Abstract Algebra*, 3rd ed. Hoboken, NJ, USA: Wiley, 2004.


**Peter G. Vouras** (M'09) received the B.A. degree in Economics and the B.A. degree in Foreign Affairs from the University of Virginia in 1989, the B.S. degree in Electrical and Computer Engineering from George Mason University in 1992, and the M.S.E. degree in Electrical and Computer Engineering from the Johns Hopkins University, Baltimore, in 2001. In March of 1996, he joined the Radar Division of the Naval Research Laboratory, Washington, DC, as an engineer and currently works in the Advanced Signal Processing Section. His research interests include adaptive array processing, multirate systems, filter banks, and radar systems engineering.

**Trac D. Tran** (S'94–M'98–SM'08–F'14) received the B.S. and M.S. degrees from the Massachusetts Institute of Technology, Cambridge, in 1993 and 1994, respectively, and the Ph.D. degree from the University of Wisconsin, Madison, in 1998, all in electrical engineering. In July of 1998, he joined the Department of Electrical and Computer Engineering, The Johns Hopkins University, Baltimore, MD, where he currently holds the rank of Professor. In the summer of 2002, he was an ASEE/ONR Summer Faculty Research Fellow at the Naval Air Warfare Center, Weapons Division at China Lake, California. Currently, he is a regular Consultant for the U.S. Army Research Laboratory, Adelphi, MD. His research interests are in the field of digital signal processing, particularly in sparse representation, sparse recovery, sampling, multirate systems, filter banks, transforms, wavelets, and their applications in signal analysis, compression, processing, and communications. His pioneering research on integer-coefficient transforms and pre-/post-filtering operators has been adopted as critical components of Microsoft Windows Media Video 9 and JPEG XR, the latest international still-image compression standard ISO/IEC 29199–2. He was the Codirector (with Prof. J. L. Prince) of the 33rd Annual Conference on Information Sciences and Systems (CISS '99), Baltimore, MD, in March 1999. He has served as an Associate Editor of the IEEE TRANSACTIONS ON SIGNAL PROCESSING as well as IEEE TRANSACTIONS ON IMAGE PROCESSING. He was a former Member of the IEEE Technical Committee on Signal Processing Theory and Methods (SPTM TC) and is a current Member of the IEEE Image Video and Multidimensional Signal Processing Technical Committee. He received the NSF CAREER Award in 2001, the William H. Huggins Excellence in Teaching Award from The Johns Hopkins University in 2007, and the Capers and Marion McDonald Award for Excellence in Mentoring and Advising in 2009.